DOI: 10.1002/marc.((insert number))

Communication

Organocatalyzed Living Radical Polymerization of Itaconates and Self-Assemblies of Rod-Coil Block Copolymers[a]

*Keling Hu, Jit Sarkar, Jie Zheng, Yan Hui Melania Lim, Atsushi Goto**

Dr. K. Hu, Dr. J. Sarkar, Dr. J. Zheng, Y. H. M. Lim, Prof. A. Goto
Division of Chemistry and Biological Chemistry, School of Physical and Mathematical Sciences, Nanyang Technological University, 21 Nanyang Link, 637371 Singapore
E-mail: agoto@ntu.edu.sg

ABSTRACT: Organocatalyzed living radical polymerizations of itaconates were studied, yielding low-dispersity linear and star polymers ($Đ = M_w/M_n$ = 1.28-1.46) up to M_n = 20000 and monomer conversion = 62%, where M_n and M_w are the number- and weight-average molar masses, respectively. The block polymerization with functional methacrylates, an acrylate, and styrene yielded various rod-coil block copolymers. Liner A-B diblock, linear B-A-B triblock, and 3-arm star A-B diblock copolymers generated spherical micelles (nano-particles) and vesicles (nano-capsules), depending on the polymer structures. Itaconates can be derived from bio-resources, and thus the obtained polymers may serve as green polymers. Because of the biocompatibility of polyitaconates, the assemblies may serve as biocompatible nano-carriers.

[a] **Supporting Information** is available online from the Wiley Online Library or from the author.

1. Introduction

A large amount of plastic is currently produced from fossil resources globally. This situation brings environmental issues and urges us to find naturally occurring substitutes to petroleum-based resources for a sustainable society.[1-4] Itaconic acid is a bio-derived vinyl monomer in radical polymerization.[5,6] It is synthesized *via* a microbial fermentation process of glucose by *Aspergillus terreus* or thermal isomerization of citric acid.[7] Itaconic acid is considered as a renewable substitute to petroleum-based acrylic acid and methacrylic acid and find applications in surfactants,[8,9] elastomers,[10,11] and so forth.[12-18] Itaconic acid is one of the 12 most promising bio-based chemicals suggested by US Department of Energy.[19] The dialkyl esters of itaconic acid such as dimethyl itaconate (DMI), diethyl itaconate (DEI), and di(*n*-butyl) itaconate (DBI) (**Figure 1**) can be synthesized *via* one-step simple esterification of itaconic acid with the corresponding alkyl alcohols (methanol, ethanol, and *n*-butanol). These alkyl alcohols are also available *via* bio-refinery of agricultural residues.[20,21] Therefore, itaconates (itaconic esters) can be considered as fully bio-based monomers. Because itaconates are α,α-disubstituted vinyl monomers, the resultant polymers are rigid polymers with large persistent lengths and tend to behave as rod-like polymers. The rod-like conformation is of interest in fundamental and practical perspectives.

Living radical polymerization,[22-25] also termed reversible-deactivation radical polymerization, was used for itaconates to synthesize well-defined polymers with predicted molar masses and narrow molar mass distributions. For example, atom transfer radical polymerization (ATRP) and reversible addition-fragmentation chain transfer (RAFT) polymerization of DMI, DBI, and dicyclohexyl itaconate successfully yielded polymers with low dispersity ($Đ = M_w/M_n$ = 1.3-1.5),[26-28] where M_n and M_w are the number- and weight-average molar masses, respectively. Because the chain transfer to monomer is generally significant for itaconates at high temperatures, the $Đ$ value tended to increase as the

polymerization proceeded.[29,30] The polymerization was also slow because of their small propagation rate constants (due to the large steric hindrance) and typically ceased at moderate monomer conversions (up to 55%).[28] Nevertheless, these results elegantly opened up the use of the bio-renewable itaconate monomers to yield structurally controlled polymers.

Our research group developed an organocatalyzed living radical polymerization exploiting alkyl iodides (R-I) as initiating dormant species and organic molecules such as tetrabutylammonium iodide (BNI (A^+I^- salt)) as catalysts.[31-35] The polymer-iodide (polymer-I) dormant species and the catalyst (iodide anion I^- in A^+I^-) form a complex (polymer-I···I^-), and the complex subsequently reversibly generates the propagating radical (polymer•) and $A^+I_2^{\bullet -}$ (**Scheme 1a**). Because $A^+I_2^{\bullet -}$ is not a stable radical, two $A^+I_2^{\bullet -}$ species can undergo disproportionation to produce A^+I^- and $A^+I_3^-$ anions, which are stable species (**Scheme 1b**). A^+I^- acts as an activator, whereas $A^+I_3^-$ acts as a deactivator (**Scheme 1c**). Polymer• can thus be deactivated by either $A^+I_2^{\bullet -}$ (**Scheme 1a**) or $A^+I_3^-$ (**Scheme 1c**). This polymerization is termed as reversible complexation mediated polymerization (RCMP). RCMP is attractive for no use of special capping agents or metal catalysts, ease of operation, and applicability to a broad scope of monomers (i.e., methacrylates, acrylates, styrene, and acrylonitrile) and polymer designs.[36-39] The present work aimed to further expand the monomer scope of RCMP to itaconates, i.e., DMI, DEI, and DBI. The use of RCMP may enable the synthesis of those bio-renewable polymers with controlled structures in a metal-free and sulfur-free condition.

Rod-coil block copolymers can form unique assembly structures and found a range of applications in composites,[40] biomaterials,[41,42] and organic electronics.[43] The rod (rigid) segment studied so far includes aromatic polymers,[44,45] π-conjugated polymers,[46,47] polypeptides,[48,49] and polyisocyanates.[50,51] Because itaconate monomers have two alkyl esters at the α-position, itaconate polymers are rigid and can be used as rod segments in rod-coil copolymers. Block copolymers with itaconate (rod) and flexible (coil) segments have

been synthesized *via* RAFT,[27] but their assembly structures have not been studied. The present paper reports the assembly structures using block copolymers synthesized *via* RCMP (**Scheme 2**). Not only a linear A-B diblock copolymer but also a linear B-A-B triblock copolymer and 3-arm stars with A-B diblock copolymer arms were studied.

2. Results and Discussion

Table 1. Polymerizations of DMI, DEI and DBI with Alkyl Iodide (R-I) Initiator, Catalyst (BNI), and Azo Initiator.

Entry	M[a)]	R-I[b)]	azo[c)]	$[M]_0/[R\text{-}I]_0/[BNI]_0/[azo]_0$ (mM)[d)]	T / °C	t / h	M_n[e)] ($M_{n,theo}$)[f)]	$Đ$[e)]	Conv / %
1	DMI	CP-I	–	8000/80/80/0 (100/1/1/0/0)	60	32	3700 (1900)	1.28	12
2	DMI	CP-I	V65	8000/80/80/60 (100/1/1/0.75)	60	48	9100 (9600)	1.42	61
3	DMI	CP-I	V65	8000/40/80/20 (200/1/2/0.5)	60	48	9900 (9600)	1.45	31
4	DMI	CP-I	V65	8000/20/80/5 (400/1/4/0.25)	60	48	16000 (12000)	1.38	19
5	DMI	CP-I	V65	8000/8/32/1.6 (1000/1/4/0.2)	60	48	20000 (16000)	1.43	10
6	DEI	EMA-I	–	8000/80/80/0 (100/1/1/0)	80	60	5600 (6000)	1.39	32
7	DEI	EMA-I	AIBN	8000/80/80/20 (100/1/1/0.25)	80	60	6200 (7800)	1.41	42
8	DBI	EMA-I	–	8000/80/80/0 (100/1/1/0)	90	60	5700 (7600)	1.40	32
9	DBI	EMA-I	V40	8000/80/80/20 (100/1/1/0.25)	90	60	6300 (9500)	1.46	39
10	DMI	EPh-II	V65	8000/40/80/50 (200/1/2/1.25)	60	48	6900 (11000)	1.39	36
11	DMI	EMA-III	V65	8000/40/120/50 (200/1/3/1.25)	60	12	11000 (6600)	1.40	62

[a] M = monomer. [b] CP-I = 2-iodo-2-methylpropionitrile, EMA-I = ethyl 2-iodo-2-methylpropionate, EPh-II = ethylene glycol bis(2-iodo-2-phenylacetate), and EMA-III = glycerol tris(2-iodoisobutyrate). [c] V65 = 2,2'-azobis(2,4-dimethylvaleronitrile), AIBN = 2,2'-azodiisobutyronitrile, and V40 = 1,1'-azobis(cyclohexane-1-carbonitrile). [d] Equivalents to R-I in the parenthesis. [e] PMMA-calibrated GPC values with tetrahydrofuran (THF) eluent. [f] Theoretical M_n values calculated according to ($[M]_0/[R\text{-}I]_0$)×(monomer conversion)×(molar mass of monomer).

2.1. Polymerizations of DMI

Figure 1 shows the alkyl-iodide initiators, catalysts, and monomers studied in this work. We first studied DMI as an itaconate monomer. We heated a mixture of DMI (100 equiv), 2-iodo-2-methylpropionitrile (CP-I) (1 equiv) as an alkyl iodide initiator, and BNI (1 equiv) as a catalyst at 60 °C (**Figure 2** (circle) and **Table 1** (entry 1)). The polymerization was slow, and the monomer conversion reached 12% after 32 h (M_n = 3700), because of the small propagation rate constant of DMI.[52,53] The $Đ$ value was relatively small, i.e., 1.28, suggesting a sufficiently high frequency of the reversible activation of polymer-I to polymer$^\bullet$ with this catalyst (BNI). All of the M_n and $Đ$ values presented in this paper are poly(methyl methacrylate) (PMMA)-calibrated gel permeation chromatography (GPC) values. They are not absolute values but are viewed as estimates. We also used other alkyl iodide initiators instead of CP-I and other organic catalysts instead of BNI (**Table S1**, Supporting Information). However, their use did not increase the monomer conversion or decrease the $Đ$ value.

An effective way to overcome the slow polymerization was the addition of an azo initiator, 2,2'-azobis(2,4-dimethylvaleronitrile) (V65) (**Figure 2** (square) and **Table 1** (entry 2)). Azo initiators are often used to decrease the deactivator concentration and hence effectively increase the polymerization rate (R_p) in living radical polymerizations.[54,55] As **Figure 2** (square) shows, the addition of V65 (0.75 equiv to R-I) dramatically increased R_p (got rid of the levelling off of the monomer conversion) even at a mild temperature 60 °C, giving a 61% monomer conversion for 48 h. The addition of V65 increased the $Đ$ value to

approximately 1.4 because of the generation of new polymer chains from V65, but the $Đ$ value was still relatively small despite the significant increase in R_p.

2.2. Chain-End Fidelity

We studied the iodide-chain-end fidelity of a poly(dimethyl itaconate)-iodide (PDMI-I) obtained in the system with V65 (**Table 1** (entry 2)) at a relatively short time of 6 h (monomer conversion = 26%) in order to minimize the effect of V65. The polymer was purified by reprecipitation in diethyl ether and subsequently with preparative GPC to remove a trace of small molecules. **Figure 3** shows the ^{1}H NMR spectrum of the PDMI-I (M_n = 4900 and $Đ$ = 1.25 after purification). As mentioned, the M_n value is not an absolute value but a PMMA-calibrated GPC value. From the initial ratio of $[DMI]_0/[CP\text{-}I]_0$ = 100 and the monomer conversion (26%), the ideal degree of polymerization (DP) is calculated to be 26, assuming that all of the polymer chains bear iodide at the chain end. Peaks *a*' (3.94-3.99 ppm) and *b*' (3.79-3.85 ppm) observed in **Figure 3** correspond to the methyl groups of the terminal monomer unit at the iodide chain end. Peaks *a* and *a*" (3.64-3.78 ppm) and *b* and *b*" (3.52-3.64 ppm) correspond to the methyl groups of the other monomer units. From the peak area ratios and the ideal DP, the iodide chain-end fidelity was estimated to be approximately 93%. A small amount of dead polymer was generated due to radical-radical termination because this polymerization is a radical polymerization. Exploiting the high chain-end fidelity, the obtained polymer (after purification) was used as a macroinitiator in the block polymerizations as shown below.

2.3. Higher Molar Masses, Other Itaconates, and Linear Di-iodide and Star-Shaped Tri-iodide Polymer Structures

For the DMI monomer, we targeted higher degrees of polymerization (DPs) of 200, 400, and 1000 at a full (100%) monomer conversion (**Table 1** (entries 3-5)). The M_n was

9900-20000 with relatively low $Đ$ values (1.38-1.45) at 10-31% monomer conversions. Besides DMI (with methyl groups), the monomer scope was extended to DEI (with ethyl groups) and DBI (with butyl groups) (**Figure 4** and **Table 1** (entries 6-9)). Because the two monomers are bulkier than DMI, the polymerizations for the two monomers were slower than that for DMI. Therefore, the optimal polymerization temperatures for DEI and DBI were 80°C and 90 °C, respectively (higher than 60 °C for DMI). A further increse in temperature was not effective because of the relatively low ceiling temperatures (T_c ~ 110 °C) of the sterically hindered itaconates.[53] The M_n value was 5600-6300 with low $Đ$ values (1.39-1.46) at 32-42% monomer conversions. We also attempted the polymerization of itaconic acid (without ester side chains) and observed no polymerization taking place, probably because the carbon-iodide chain end decomposed via an acid-catalyzed HI elimination.

For the DMI monomer, we also studied the use of alkyl di-iodide (EPh-II) and alkyl tri-iodide (EMA-III) dormant species (**Table 1** (entries 10 and 11)), yielding linear di-iodide and star-shaped tri-iodide polymers with M_n = 6900-11000 and $Đ$ = 1.39-1.40.

Table 2. Polymerizations of DMI, DEI, and DBI Using In Situ Formed Alkyl Iodide.

Entry	**M**[a]	**$[M]_0/[I_2]_0/[V65]_0/[BNI]_0$ (mM)**[b]	***T* / °C**	***t* / h**	**M_n**[c] **($M_{n,theo}$)**[d]	**$Đ$**[c]	**Conv / %**
1	DMI	8000/40/120/80 (100/0.5/1.5/1)	60	48	9400 (9900)	1.37	63
2	DEI	8000/40/120/80 (100/0.5/1.5/1)	60	48	5900 (7900)	1.54	43
3	DBI	8000/40/120/80 (100/0.5/1.5/1)	60	48	6100 (9000)	1.58	37

[a] M = monomer. [b] V65 = 2,2'-azobis(2,4-dimethylvaleronitrile)**.** Equivalents to twice of I_2 in the parenthesis. [c] PMMA-calibrated GPC values with tetrahydrofuran (THF) eluent. [d] Theoretical M_n values calculated according to $([M]_0/(2\times[I_2]_0))\times$(monomer conversion)×(molar mass of monomer).

2.4. Use of Alkyl Iodide Formed In Situ

Instead of a preformed isolated alkyl iodide (e.g., CP-I studied above), we can employ molecular iodine (I_2) and an azo compound (R-N=N-R) as the starting compounds; then, the R-I formed *in situ* can be used for the polymerization. The I_2/azo method was originally developed by Lacroix-Desmazes et al. for iodide-transfer polymerization (ITP)[56,57] and subsequently used in RCMP.[32] This method is practically attractive because of no necessity of the isolation or purification of the alkyl iodide. Here, we use this method for the RCMPs of itaconates.

Figure 2 (triangle) and **Table 2** (entry 1) show the polymerization of DMI (100 equiv) with V65 (1.5 equiv), I_2 (0.5 equiv), and BNI (1 equiv) at 60 °C. V65 affords the alkyl radical $R^{\bullet}$, which reacts with I_2 to yield R-I. Virtually no polymerization occurred for 2 h, during which time $R^{\bullet}$ predominantly reacted with I_2 (rather than the monomer), and R-I accumulated. Because the efficiency of V65 to produce free $R^{\bullet}$ is not unity but approximately 0.6-0.7, an approximately 0.75 equivalent of V65 was used to consume the 0.5 equivalent I_2 to generate 1 equivalent of R-I in the present system. After this period (2 h), the polymerization proceeded by the catalytic work of BNI and the continuous supply of radicals from the remaining amount of V65 (0.75 equiv). The conversion reached 63% for 48 h, yielding a low-dispersity polymer (M_n = 9400 and $Đ$ = 1.37). This method was also effective for the other two monomers, i.e., DEI and DBI (**Table 2** (entries 2 and 3)).

Table 3. Diblock Polymerizations from PDMI-I and PMMA-I.

Entry	M[a)]	R-I[b)]	Azo[c)]	$[M]_0/[R\text{-}I]_0/[BNI]_0/[azo]_0$ (mM)[d)]	T / °C	t / h	M_n[e)] ($M_{n,theo}$)[f)]	$Đ$[e)]	Conv / %
1	MMA	PDMI-I	–	8000/11/45/0 (700/1/4/0)	70	16	82000 (60000)	1.30	77
2	BzMA	PDMI-I	AIBN	8000/20/80/4 (400/1/4/0.2)	70	12	95000 (66000)	1.36	85
3	PEGMA[g)]	PDMI-I	V65	8000/20/160/4[h)] (400/1/8/0.2)	50	24	87000 (34000)	1.49	24
4	MTEMA	PDMI-I	AIBN	8000/20/40/4 (400/1/2/0.2)	70	27	46000 (60000)	1.45	86
5	TFEMA	PDMI-I	AIBN	8000/13/27/2.7[i)] (600/1/2/0.2)	70	30	130000 (86000)	1.39	77
6	PA	PDMI-I	–	8000/12/50/0 (650/1/4/0)	110	25	39000 (32000)	1.44	28
7	St	PDMI-I	AIBN	8000/13/27/5 (600/1/2/0.4)	80	14	56000 (42000)	1.46	57
8	DMI	PMMA-I	–	8000/40/80/0 (200/1/2/0)	60	16	8800 (8400)	1.28	14

[a)] M = monomer. [b)] PDMI-I with M_n = 5800 and $Đ$ = 1.27 for entries 1 and 2, M_n = 4300 and $Đ$ = 1.26 for 3 and 5, M_n = 4900 and $Đ$ = 1.25 for entries 4 and 6, and M_n = 5200 and $Đ$ = 1.15 for entry 7. PMMA-I with M_n = 3700 and $Đ$ = 1.14 for entry 8. [c)] V65 = 2,2'-azobis(2,4-dimethylvaleronitrile) and AIBN = 2,2'-azodiisobutyronitrile. [d)] Equivalents to R-I in the parenthesis. [e)] PMMA-calibrated GPC values with tetrahydrofuran (THF) eluent. [f)] Theoretical M_n values calculated according to (molar mass of R-I)+($[M]_0/[R\text{-}I]_0$)×(monomer conversion)×(molar mass of monomer). [g)] Molar mass of PEGMA = 300. [h)] ONI as catalyst instead of BNI. [i)] Diglyme = 50 wt% (solution polymerization).

2.5. Block Polymerizations

Exploiting the high iodide-chain end fidelity, the mentioned PDMI-I (M_n = 4900 and $Đ$ = 1.25 after purification) was used as a macroinitiator to obtain rod-coil block copolymers. For the second block (coil) segment, we used various functional methacrylates with methyl (MMA), benzyl (BzMA), poly(ethylene glycol) methyl ether (PEGMA, molar mass = 300), 2,2,2-trifluoroethyl (TFEMA), and 2-(methylthio)ethyl (MTEMA) groups, an acrylate with

phenyl (PA) group, and styrene (St) (**Figure 1**). The polymerization temperature was 50-70 °C for the methacrylates, 110 °C for the acrylate, and 80 °C for St. In all cases, a large fraction of PDMI-I smoothly extended (**Figure 5**), successfully yielding rod-coil block copolymers with hydrophobic, amphiphilic, and super-hydrophobic coil segments (**Table 3** (entries 1-7)). The observed small amount of the remaining macroinitiator also in turn confirms the high iodide-chain-end fidelity of the PDMI-I macroinitiator. The macroinitiators used in **Table 3** (entries 1-7) were synthesized in a few different batches and hence had slightly different M_n (= 4300-5800) and $Đ$ (= 1.15-1.27) values.

We also synthesized a PMMA-I (M_n = 3700 and $Đ$ = 1.14 after purification) and used it as a macroinitiator in the polymerization of DMI (**Table 3** (entry 8) and **Figure 5h**). PMMA-I smoothly extended. The PMMA-PDMI block copolymers were obtained in both directions from PDMI-I (**Table 3** (entry 1) and **Figure 5a**) and PMMA-I (**Table 3** (entry 8) and **Figure 5h**).

As mentioned, most of the reported rod-coil block copolymers contain polyaromatic, polyamide, and polyisocyanate rod segments accessible *via* non-radical-polymerization such as polycondensation. Therefore, the block copolymers were synthesized *via* the rod segment synthesis (polycondensation), the coil-segment synthesis (radical polymerization), and the additional step to couple the two segments.[58] Unlike such three-step synthesis, the use of polyitaconates in the rod segment requires only two consecutive radical polymerization steps to obtain rod-coil block copolymers. The use of itaconates reduces the synthetic step and also broadens the family of rod-coil copolymers.

Table 4. Self-Assembly Behaviors of PDMI-PPEGMA Block Copolymers.

Entry	Block Copolymer[a)]	M_n[b)]	$Đ$[b)]	Hydrodynamic diameter (nm)[c)]	DLS size distribution index	Assembly structure[d)]
1	$PDMI_{28}$-$PPEGMA_7$	6600	1.20	122	0.22	S
2	$PPEGMA_3$-$PDMI_{28}$-$PPEGMA_3$	6400	1.14	190	0.23	V
3	3-arm $PDMI_{20}$-$PPEGMA_3$	12000	1.21	79	0.14	S
4	3-arm $PDMI_{20}$-$PPEGMA_5$	14000	1.26	79	0.20	S
5	3-arm $PDMI_{20}$-$PPEGMA_9$	17000	1.31	68	0.23	S

[a)] The DPs of the PDMI and PMMA segments were not absolute values but were estimated from the M_n values obtained by PMMA-calibrated GPC values with tetrahydrofuran (THF) eluent. [b)] PMMA-calibrated GPC values with THF eluent. [c)] The DLS peak top value. [d)] S = spherical micelle and V = vesicle.

2.6. Self-Assembly Behaviour

As shown in **Table 3** (entry 3), we can obtain a block copolymer containing a water-insoluble PDMI rod segment and a water-soluble PPEGMA coil segment, where PPEGMA is poly(poly(ethylene glycol) methyl ether methacrylate). Because of the amphiphilic nature, PDMI-PPEGMA block copolymers may form self-assemblies in water. PPEGMA is bio-compatible, and PDMI has also been demonstrated to be biocompatible.[59] Therefore, the self-assemblies of PDMI-PPEGMA block copolymers may serve as very suitable carriers in biological applications.

We studied the self-assemblies of three topologically different PDMI-PPEGMA block copolymers, i.e., a linear A-B diblock copolymer ($PDMI_{28}$-$PPEGMA_7$), a linear B-A-B triblock copolymer ($PPEGMA_3$-$PDMI_{28}$-$PPEGMA_3$), and a 3-arm star with A-B diblock copolymer arms (three $PDMI_{20}$-$PPEGMA_5$ arms), where the number given in the subscript is

the DP of the segment. The weight fraction of PDMI (f_{PDMI}) was fixed to approximately 68-71%. These polymers were synthesized using alkyl mono-iodide (CP-I), alkyl di-iodide (EPh-II), and alkyl tri-iodide (EMA-III) (**Figure 1**), respectively, *via* the block polymerizations of DMI (first block) and PEGMA (second block) (**Table 4** (entries 1, 2, and 4)). The successful synthesis of the 3-arm star block copolymer was confirmed by smooth chain extension from the 3-arm macroinitiator (**Figure S1**). The polymer was dissolved in a small amount of tetrahydrofuran (THF) and then added into deionized water (1 wt% polymer in 99% solvent (THF/water = 1/9)). (We also studied a lower concentration of polymer (0.1 wt% polymer in 99.9% solvent (THF/water = 1/9)) and observed similar assembly structures.)

The dynamic light scattering (DLS) analysis (**Figure 6a**) showed the formation of an assembly with a peak-top diameter of 122 nm, 190 nm, and 79 nm for the linear A-B diblock, linear B-A-B triblock, and 3-arm star A-B diblock copolymers, respectively (**Table 4** (entries 1, 2, and 4)). **Figure 6b** (A, B, and C) shows the transmission electron microscopy (TEM) images of the self-assemblies. Interestingly, despite approximately the same f_{PDMI} values, the linear A-B diblock copolymer formed spherical micelles (**Figure 6b** (A)), the linear B-A-B triblock copolymer formed vesicles (**Figure 6b** (B)), and the 3-arm star A-B diblock copolymer formed spherical micelles (**Figure 6b** (C)). Thus, the self-assembly morphologies depended on the polymer topologies.

For the linear diblock copolymer, the contour end-to-end length of is 9 nm (= 0.25 nm × (28 + 7) units). The particle size (122 nm) was much larger than twice of the contour length (18 nm = 2 × 9 nm), meaning that the observed spherical micelle is not a normal core-shell micelle. A possible structure is a large compound micelle, for example.

The liner triblock copolymer bears a water-soluble polymer (PPEGMA) at the two outer segments and can form monolayer vesicles. The water-insoluble PDMI segment is rigid and would be aligned with efficient space-filling, which would be a driving force to give a small curvature and hence form vesicles. The vesicle formation would be a unique feature of

the rigidity of the PDMI segment in the triblock copolymer. The contour end-to-end length of is 8.5 nm (= 0.25 nm × (3 + 28 + 3) units). The particle size (190 nm) was much larger than twice of the contour length (17 nm = 2 × 8.5 nm), which is not contradictory to the vesicle structure.

The star copolymer has a larger M_n value (= 14000) than the linear diblock copolymer (M_n = 6600), while the f_{PDMI} values are almost the same. The particle size (79 nm) for the star was smaller than that (122 nm) for the liner diblock. For the star copolymer, the contour end-to-end length of the two arms is 12.5 nm (= 0.25 nm × ((20 + 5) × 2 units)). The particle size (79 nm) was still much larger than twice of the contour length (25 nm = 2×14 nm), again meaning that the observed micelle is not a normal core-shell micelle but another morphology such as a large compound micelle.

Additionally, we also studied the star copolymers with shorter (3 units) and longer (9 units) PPEGMA segments at the same length (20 units) of the PDMI segment. The TEM images (**Figure 6b** (D and E)) showed the formation of spherical micelles from both star polymers similarly to the star with 5 units of the PPEGMA segment (**Figure 6b** (C)). The particle size tended to be smaller with an increase in the units of the PPEGMA segment (79 nm for 3 units and 5 units, and 69 nm for 9 units).

3. Conclusions

The RCMP of itaconates, i.e., DMI, DEI, and DBI, successfully yielded low-dispersity linear and star polymers ($Đ$ = 1.28-1.46) up to M_n = 20000 and monomer conversion = 62%. Rod-coil block copolymers of DMI and various functional methacrylates, an acrylate, and styrene were obtained with high block efficiencies. The use of itaconates requires only two consecutive radical polymerization steps to obtain rod-coil block copolymers unlike other three-step systems and also broadens the family of rod-coil copolymers. Itaconates can be

derived from bio-resources, and thus the obtained polymers may serve as green polymers. We successfully obtained spherical micelles (nano-particles) from the linear and 3-arm A-B diblock copolymers and vesicles (nano-capsules) from the linear B-A-B triblock copolymer. Because of the biocompatibility of the polyitaconates, those assemblies may serve as biocompatible nano-carriers. The rod-coil polymers may also find applications for liquid crystals and fillers of polymer composites.

Supporting Information

Supporting Information is available from the Wiley Online Library or from the author ((delete if necessary))

Appendix/Nomenclature/Abbreviations

This work was supported by Industry alignment fund - pre-positioning programme (IAF-PP) (M4070277) of Agency for Science, Technology and Research (A*STAR) in Singapore.

Received: Month XX, XXXX; Revised: Month XX, XXXX; Published online:
((For PPP, use "Accepted: Month XX, XXXX" instead of "Published online")); DOI:
10.1002/marc.((insert number)) ((or ppap., mabi., macp., mame., mren., mats.))

Keywords: itaconates, rod-coil block copolymers, self-assembly, organocatalyzed living radical polymerization

[1] Y. Zhu, C. Romain, C. K. Williams, *Nature* **2016**, *540*, 354.

[2] S. Lambert, M. Wagner, *Chem. Soc. Rev.* **2017**, *46*, 6855.

[3] G. John, S. Nagarajan, P. K. Vemula, J. R. Silverman, C.K.S. Pillai, *Prog. Polym. Sci.* **2019**, *92*, 158.

[4] Z. Wang, M. S. Ganewatta, C. Tang, *Prog. Polym. Sci.* **2020**, *101*, 101197.

[5] S. Bednarz, A. Błaszczyk, D. Błazejewska, D. Bogdał, *Catalysis Today* **2015**, *257*, 297.

[6] J. T. Trotta, M. Jin, K. J. Stawiasz, Q, Michaudel, W.-L. Chen, B. P. Fors, *J. Polym. Sci., Part A: Polym. Chem.* **2017**, *55*, 2730.

[7] T. Willke, K. D. Vorlop, *Appl. Microbiol. Biotechnol.* **2001**, *56*, 289.

[8] D. Malferrari, N. Armenise, S. Decesari, P. Galletti, E. Tagliavini, *ACS Sustainable Chem. Eng.* **2015**, *3*, 1579.

[9] S. Chakraborty, S. Ramakrishnan, *Langmuir* **2018**, *34*, 11729.

[10] K. Satoh, D.-H. Lee, K. Nagai, M. Kamigaito, *Macromol. Rapid Commun.* **2014**, *35*, 161.

[11] R. Wang, J. Ma, X. Zhou, Z. Wang, H. Kang, L. Zhang, K. Hua, J. Kulig, *Macromolecules* **2012**, *45*, 6830.

[12] T. Okuda, K. Ishimoto, H. Ohara, S. Kobayashi, *Macromolecules* **2012**, *45*, 4166.

[13] A. Bohre, M. A. Ali, M. Ocepek, M. Grilc, J. Zabret, B. Likozar, *Ind. Eng. Chem. Res.* **2019**, *58*, 19825.

[14] S. Ma, X. Liu, L. Fan, Y. Jiang, L. Cao, Z. Tang, J. Zhu, *ChemSusChem* **2014**, *7*, 555.

[15] A. M. Medway, J. Sperry, *Green Chem.* **2014**, *16*, 2084.

[16] S. Bonardd, A. Alegria, C. Saldias, A. Leiva, G. Kortaberria, *ACS Appl. Mater. Interfaces* **2018**, *10*, 38476.

[17] J. T. Trotta, A. Watts, A. R. Wong, A. M. LaPointe, M. A. Hillmyer, B. P. Fors, *ACS Sustainable Chem. Eng.* **2019**, *7*, 2691.

[18] Z. Dai, Z. Yang, Z. Chen, Z. Zhao, Y. Lou, Y. Zhang, T. Liu, F. Fu, Y. Fu, X. Liu, *ACS Sustainable Chem. Eng.* **2018**, *6*, 15056.

[19] A. Lv, Z.-L. Li, F.-S. Du, Z.-C. Li, *Macromolecules* **2014**, *47*, 7707.

[20] A. ElMekawy, L. Diels, H. D. Wever, D. Pant, *Environ. Sci. Technol.* **2013**, *47*, 9014.

[21] P. N. R. Vennestrøm, C. M. Osmundsen, C. H. Christensen, E. Taarning, *Angew. Chem. Int. Ed.* **2011**, *50*, 10502.

[22] K. Matyjaszewski, *Adv. Mater.* **2018**, *30*, 1706441.

[23] K. Matyjaszewski, N. V. Tsarevsky, *J. Am. Chem. Soc.* **2014**, *136*, 6513.

[24] J. Nicolas, Y. Guillaneuf, C. Lefay, D. Bertin, D. Gigmes, B. Charleux, *Prog. Polym. Sci.* **2013**, *38*, 63.

[25] D. J. Keddie, G. Moad, E. Rizzardo, S. H. Thang, *Macromolecules* **2012**, *45*, 5321.

[26] M. Fernández-García, M. Fernández-Sanz, J. L. de la Fuente, E. L. Madruga, *Macromol. Chem. Phys.* **2001**, *202*, 1213.

[27] Z. Szablan, A. A. Toy, T. P. Davis, X. Hao, M. H. Stenzel, C. Barner-Kowollik, *J. Polym. Sci., Part A: Polym. Chem.* **2004**, *42*, 2432.

[28] Z. Szablan, A. A. Toy, A. Terrenoire, T. P. Davis, M. H. Stenzel, A. H. E. Müller, C. Barner-Kowollik, *J. Polym. Sci., Part A: Polym. Chem.* **2006**, *44*, 3692.

[29] G. E. Roberts, T. P. Davis, J. P. A. Heuts, *Macromolecules* **2002**, *35*, 9954.

[30] T. Hirano, R. Takeyoshi, M. Seno, T. Sato, *J. Polym. Sci., Part A: Polym. Chem.* **2002**, *40*, 2415.

[31] A. Goto, T. Suzuki, H. Ohfuji, M. Tanishima, T. Fukuda, Y. Tsujii, H. Kaji, *Macromolecules* **2011**, *44*, 8709.

[32] A. Goto, A. Ohtsuki, H. Ohfuji, M. Tanishima, H. Kaji, *J. Am. Chem. Soc.* **2013**, *135*, 11131.

[33] A. Ohtsuki, L. Lei, M. Tanishima, A. Goto, H. Kaji, *J. Am. Chem. Soc.* **2015**, *137*, 5610.

[34] C.-G. Wang, A. Goto, *J. Am. Chem. Soc.* **2017**, *139*, 10551.

[35] H. Xu, C.-G. Wang, Y. Lu, A. Goto, *Macromolecules* **2019**, *52*, 2156.

[36] J. Zheng, C.-G. Wang, Y. Yamaguchi, M. Miyamoto, A. Goto, *Angew. Chem. Int. Ed.* **2018**, *57*, 1552.

[37] C.-G. Wang, C. Chen, K. Sakakibara, Y. Tsujii, A. Goto, *Angew. Chem. Int. Ed.* **2018**, *57*, 13504.

[38] X. Liu, C.-G. Wang, A. Goto, *Angew. Chem. Int. Ed.* **2019**, *58*, 5598.

[39] J. Zheng, C. Chen, A. Goto, *Angew. Chem. Int. Ed.* **2020**, *59*, 1941.

[40] B. D. Olsen, R. A. Segalman, *Materials Science and Engineering R* **2008**, *62*, 37.

[41] J. Zhang, X.-F. Chen, H.-B. Wei, X.-H. Wan, *Chem. Soc. Rev.* **2013**, *42*, 9127.

[42] D. Wu, Y. Huang, F. Xu, Y. Mai, D. Yan, *J. Polym. Sci., Part A: Polym. Chem.* **2017**, *55*, 1459.

[43] C.-L. Liu, C.-H. Lin, C.-C. Kuo, S.-T. Lin, W.-C. Chen, *Progress in Polymer Science* **2011**, *36*, 603.

[44] M. Koga, K. Abe, K. Sato, J. Koki, S. Kang, K. Sakajiri, J. Watanabe, M. Tokita *Macromolecules* **2014**, *47*, 4438.

[45] Y. Yang, K. Zhong, T. Chen, L. Y. Jin, *Langmuir* **2018**, *34*, 10613.

[46] S. Yu, Y. Yang, T. Chen, J. Xu, L. Y. Jin, *Nanoscale* **2017**, *9*, 17975.

[47] Y. Huang, Y. Mai, X. Yang, U. Beser, J. Liu, F. Zhang, D. Yan, K. Müllen, X. Feng, *J. Am. Chem. Soc.* **2015**, *137*, 11602.

[48] C. Cai, J. Lin, Y. Lu, Q. Zhang, L. Wang, *Chem. Soc. Rev.* **2016**, *45*, 5985.

[49] H. Tran, Y. Zhang, C. K. Ober, *ACS Macro Lett.* **2018**, *7*, 1186.

[50] X. Liu, J. Deng, Y. Wu, L. Zhang, *Polymer* **2012**, *53*, 5717.

[51] P. N. Shah, J. Min, H.-J. Kim, S.-Y. Park, J.-S. Lee, *Macromolecules* **2011**, *44*, 7917.

[52] T. Otsu, K. Yamagishi, A. Matsumoto, M. Yoshioka, H. Watanabe, *Macromolecules* **1993**, *26*, 3026.

[53] Z. Szablan, M. H. Stenzel, T. P. Davis, L. Barner, C. Barner-Kowollik, *Macromolecules* **2005**, *38*, 5944.

[54] A. Goto, T. Fukuda, *Prog. Polym. Sci.* **2004**, *29*, 329.

[55] H. Fischer, *Chem. Rev.* **2001**, *101*, 3581.

[56] P. Lacroix-Desmazes, R. Severac, B. Boutevin, *Macromolecules* **2005**, *38*, 6299.

[57] C. Boyer, P. Lacroix-Desmazes, J.-J. Robin, B. Boutevin, *Macromolecules* **2006**, *39*, 4044.

[58] S.-H. Lin, S.-J. Wu, C.-C. Ho, W.-F. Su, *Macromolecules* **2013**, *46*, 2725.

[59] D. G. Barrett, T. J. Merkel, J. C. Luft, M. N. Yousaf, *Macromolecules* **2010**, *43*, 9660.

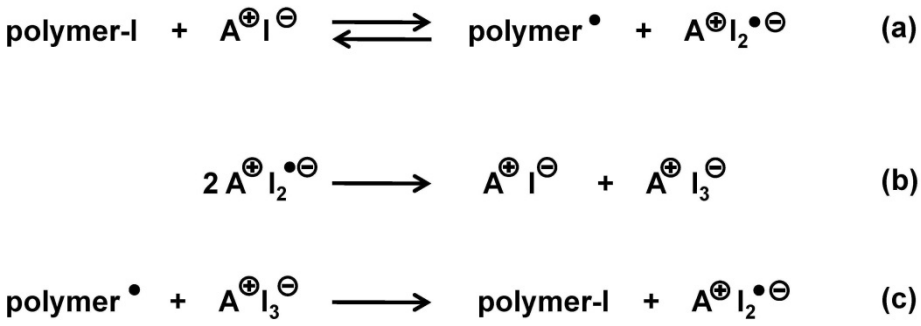

Scheme 1. Reversible activation of RCMP.

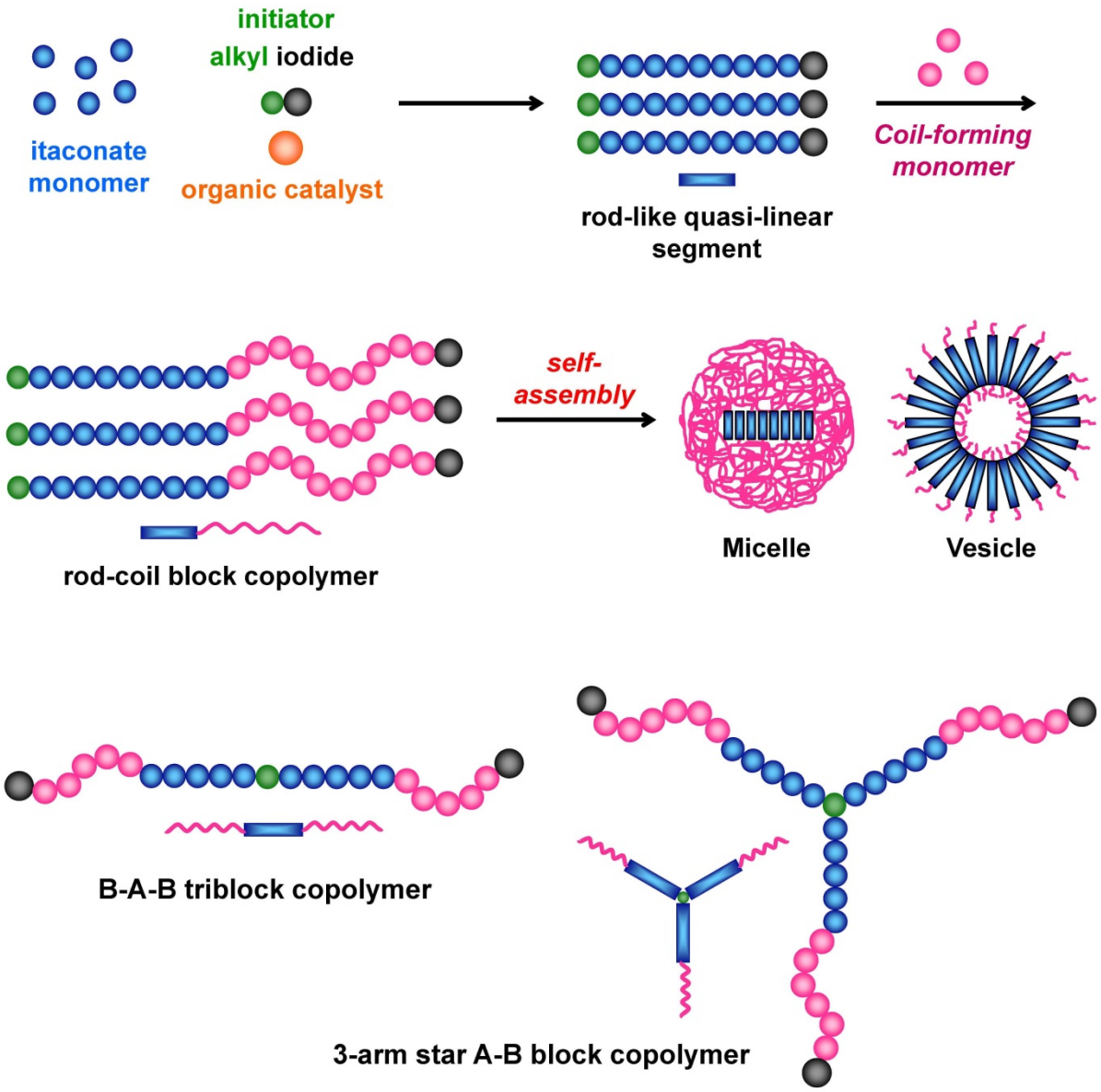

Scheme 2. RCMP of itaconate, synthesis of rod-coil block copolymer, and its self-assemblies.

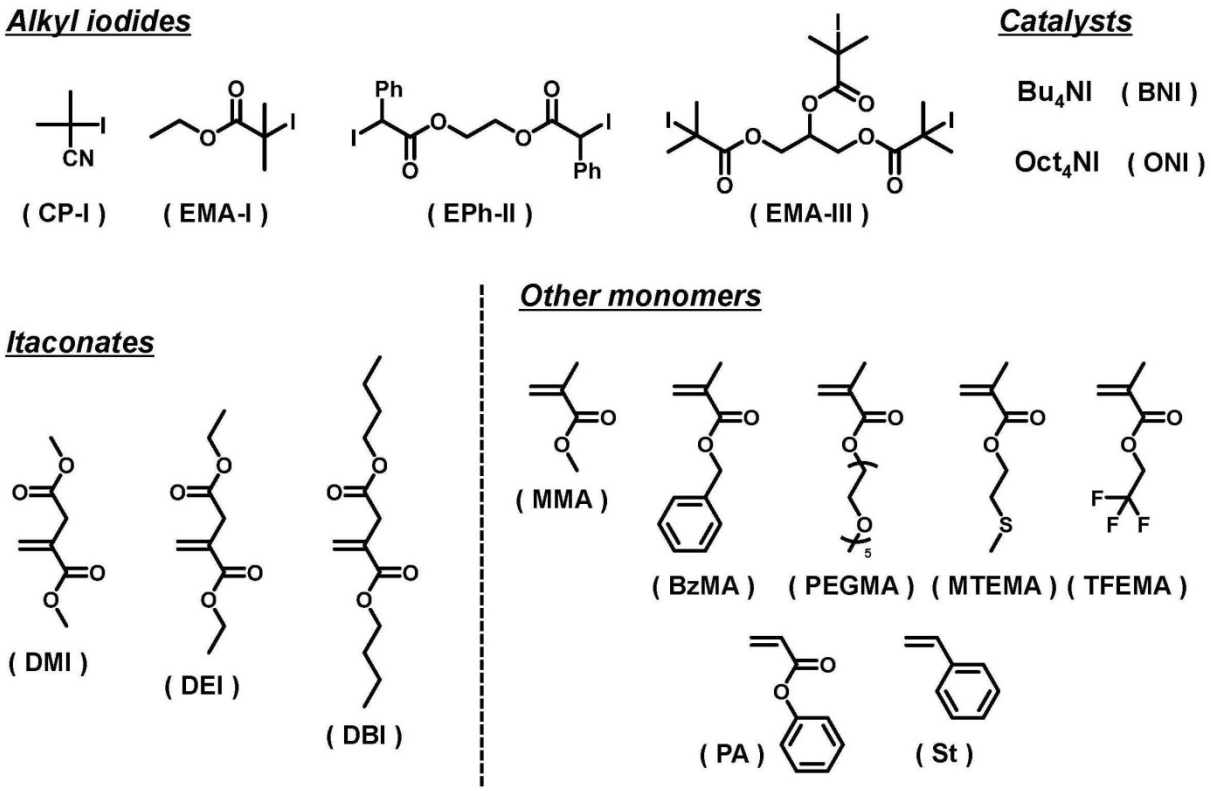

Figure 1. Structures of alkyl iodide initiators, catalysts, and monomers studied in this work.

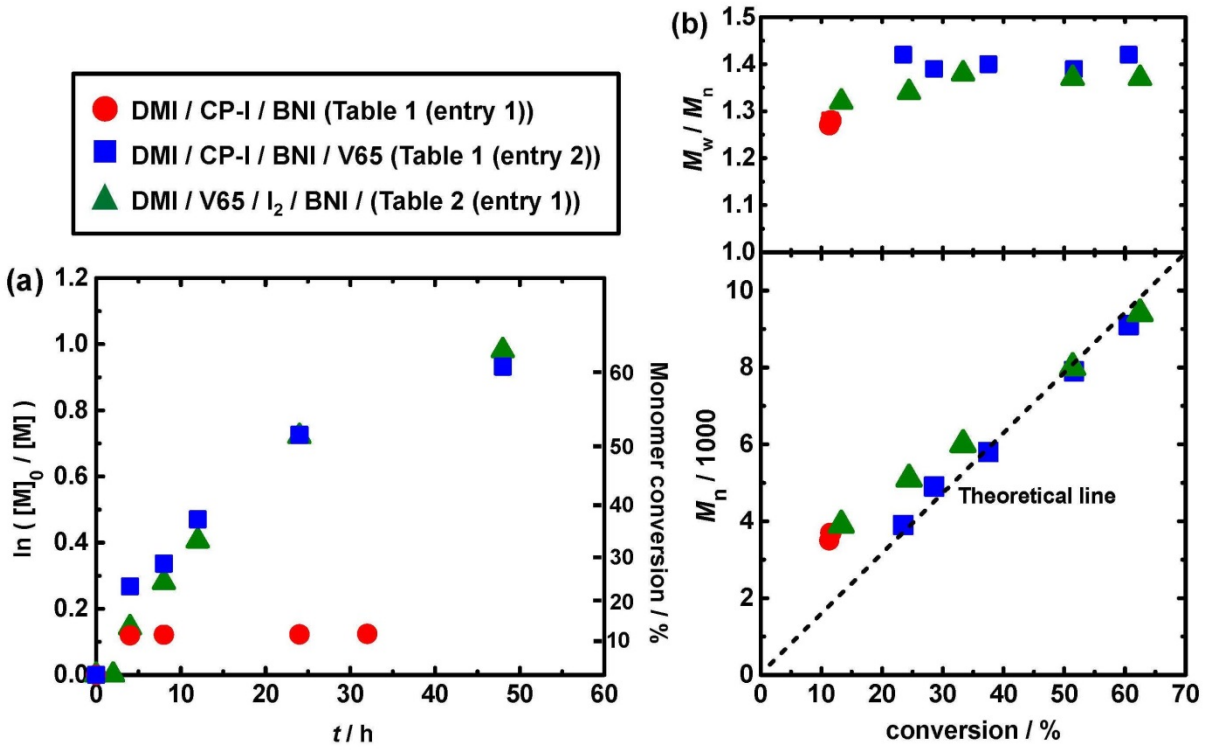

Figure 2. Plots of (a) $\ln([M]_0/[M])$ vs t and (b) M_n and M_w/M_n vs conversion for the DMI/CP-I/BNI/V65 system (60 °C): $[DMI]_0$ = 8 M; $[CP\text{-}I]_0$ = 80 mM; $[BNI]_0$ = 80 mM; $[V65]_0$ = 0 or 60 mM, and for the DMI/V65/I_2/BNI system (60 °C): $[DMI]_0$ = 8 M; $[V65]_0$ = 120 mM; $[I_2]_0$ = 40 mM; $[BNI]_0$ = 80 mM. The symbols are indicated in the figure.

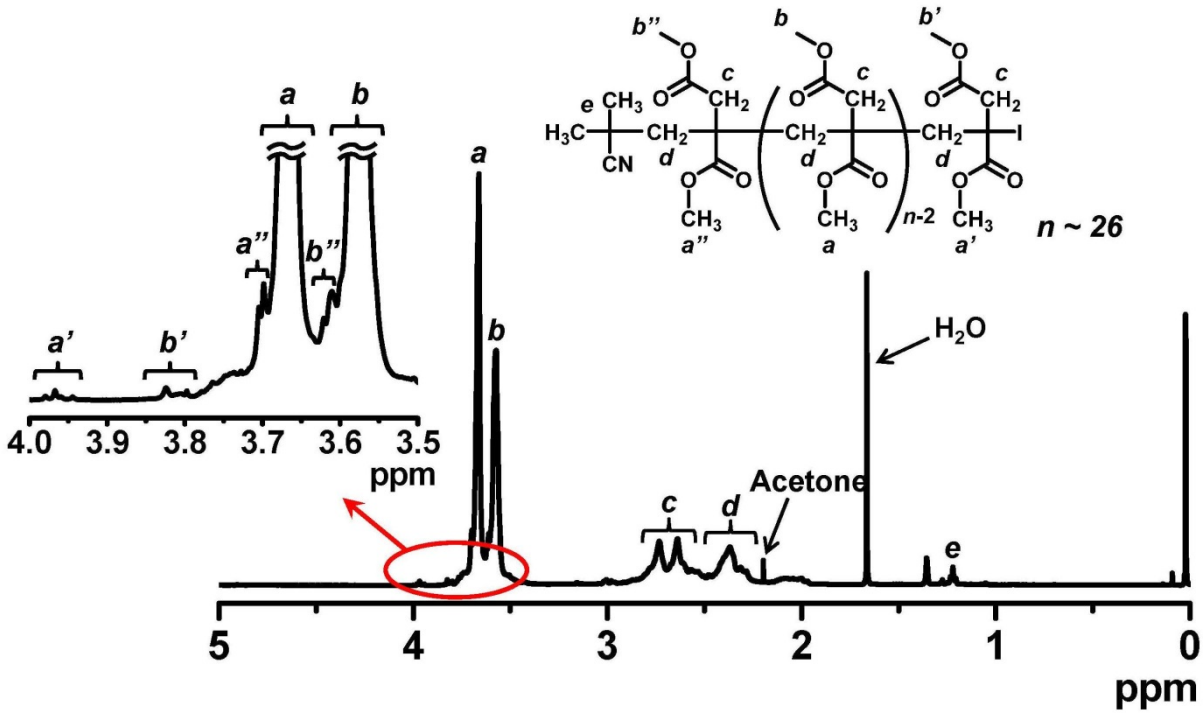

Figure 3. ^{1}H NMR spectrum ($CDCl_3$) of PDMI-I obtained in the polymerization shown in Table 1 (entry 2) for 6 h (M_n = 4900 and $Đ$ = 1.25 after purification).

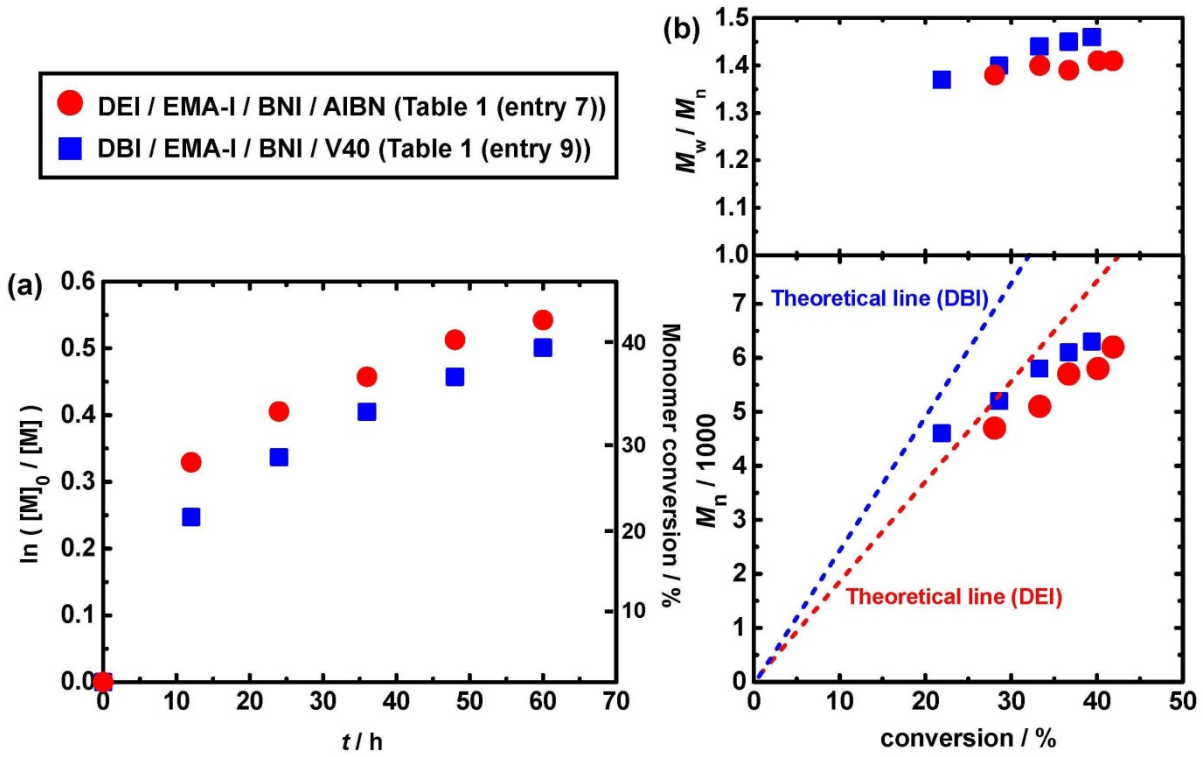

Figure 4. Plots of (a) ln([M]$_0$/[M]) vs t and (b) M_n and M_w/M_n vs conversion for the DEI/EMA-I/BNI/AIBN system in bulk (80 °C): [DEI]$_0$ = 8 M; [EMA-I]$_0$ = 80 mM; [BNI]$_0$ = 80 mM; [AIBN]$_0$ = 20 mM, and for the DBI/EMA-I/BNI/V40 system in bulk (90 °C): [DBI]$_0$ = 8 M; [EMA-I]$_0$ = 80 mM; [BNI]$_0$ = 80 mM; [V40]$_0$ = 20 mM. The symbols are indicated in the figure.

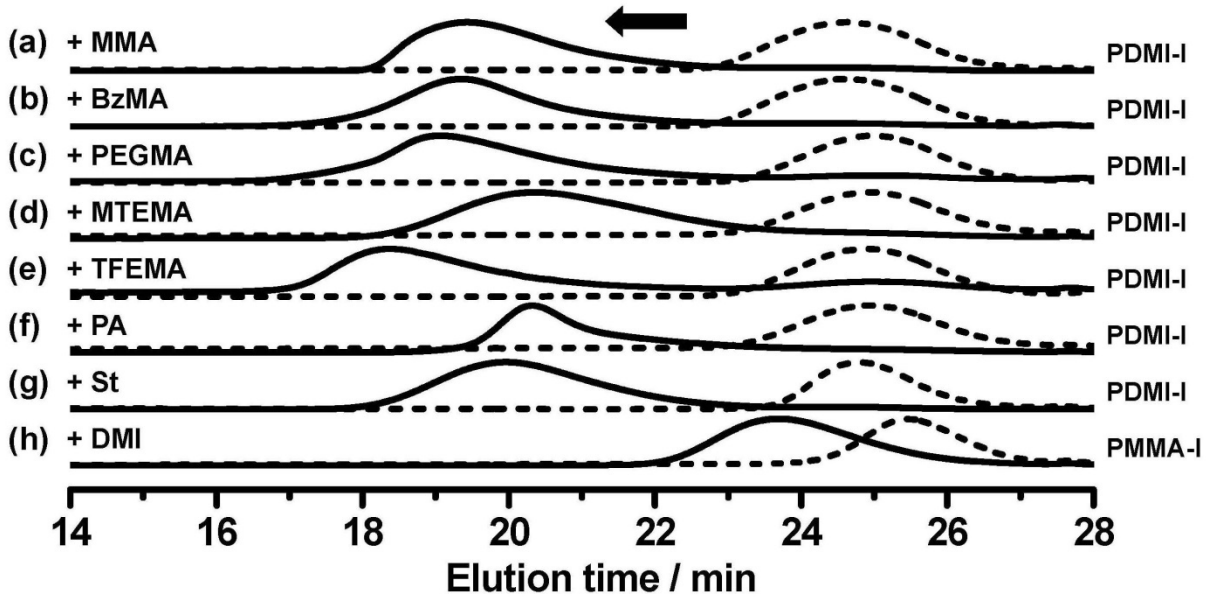

Figure 5. GPC chromatograms before (dashed lines) and after (solid lines) the block polymerizations in Table 3. (a)-(h) corresponds to entries 1-8 in Table 3, respectively.

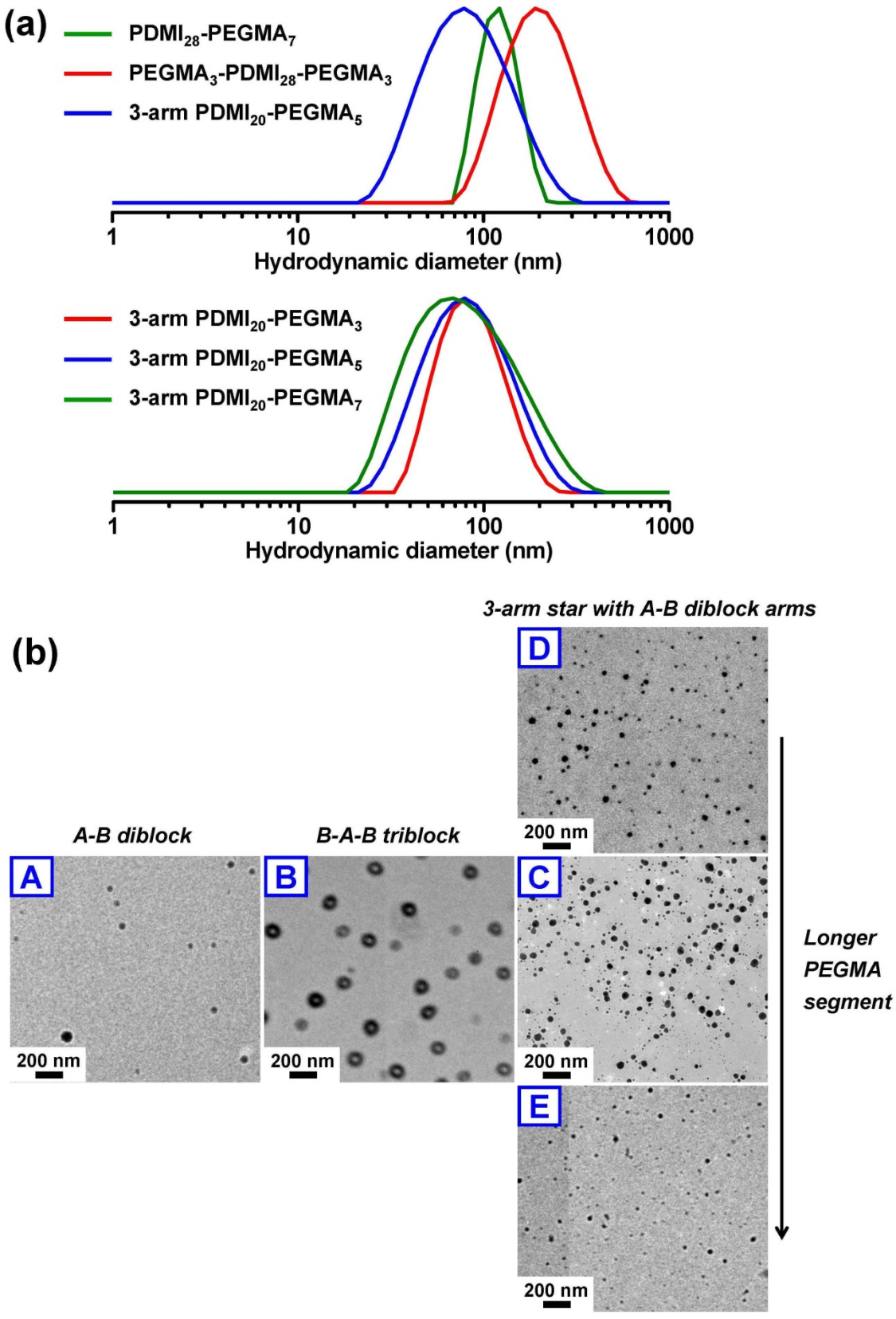

Figure 6. Self-assembly of PDMI-PPEGMA block copolymers (Table 4) in an aqueous solution (1 wt% polymer in THF/water = 1/9). (a) DLS curves and (b) TEM images of the obtained assemblies. The symbols are indicated in the figures.

The table of contents entry

K. L. Hu, J. Sarkar, J. Zheng, Y. H. M. Lim, A. Goto*

Organocatalyzed Living Radical Polymerization of Itaconates and Self-Assemblies of Rod-Coil Block Copolymers

Organocatalyzed living radical polymerizations of itaconates yielded low-dispersity linear and star polymers. Liner A-B diblock, linear B-A-B triblock, and 3-armed star A-B diblock rod-coil copolymers generated spherical micelles and vesicles, depending on the polymer structures. Itaconates can be derived from bio-resources, and the obtained polymers may serve as green polymers.

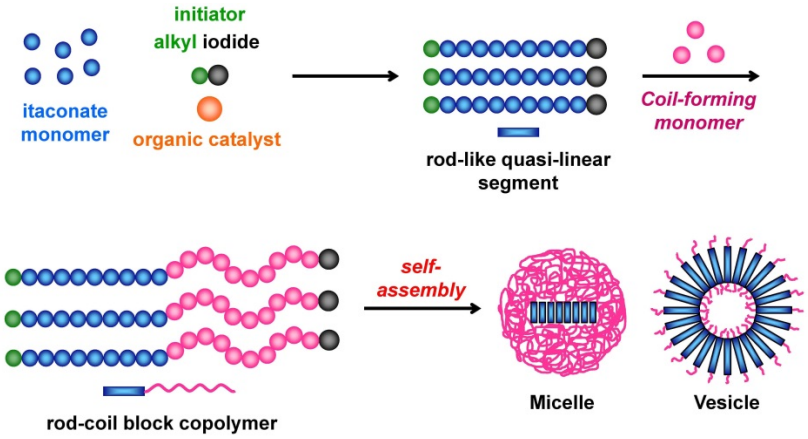

((Supporting Information should be included here for submission only; for publication, please provide Supporting Information as a separate PDF file.))

Supporting Information

for *Macromol. Rapid Commun.*, DOI: 10.1002/marc.2013#####

Organocatalyzed Living Radical Polymerization of Itaconates and Self-Assemblies of Rod-Coil Block Copolymers

Keling Hu, Jit Sarkar, Jie Zheng, Yan Hui Melania Lim, Atsushi Goto*

1. Experimental

Materials. Dimethyl itaconate (DMI) (> 98%, Tokyo Chemical Industry (TCI), Japan), diethyl itaconate (DEI) (>98%, TCI), dibutyl itaconate (DBI) (>97%, TCI), 2-iodo-2-methylpropionitrile (CP-I) (>95%, TCI), ethyl *α*-iodophenylacetate (EPh-I) (>98%, TCI), ethyl 2-iodo-2-methylpropionate (EMA-I) (>94%, TCI), tetrabutylammonium iodide (BNI) (>98%, TCI), tetra-*n*-octylammonium iodide (ONI) (>98%, TCI), tributylmethylphosphonium iodide (BMPI) (>98%, TCI), acetylcholine iodide (AChI) (>98%, TCI), butyrylcholine iodide (BChI) (>99%, TCI), methyl methacrylate (MMA) (>99.8%, TCI), benzyl methacrylate (BzMA) (>98%, TCI), poly(ethylene glycol) methyl ether methacrylate (PEGMA) (average M_n = 300, Sigma-Aldrich, United States), 2-(methylthio)ethyl methacrylate (MTEMA) (96%, Sigma-Aldrich), 2,2,2-trifluoroethyl methacrylate (TFEMA) (>98%, TCI), phenyl acrylate (PA) (>98%, TCI), styrene (St) (>99%, TCI), 2,2'-azobis(2,4-dimethylvaleronitrile) (V65) (95%, Wako Pure Chemical, Japan), 2.2′-azobis(2-methylpropionitrile) (AIBN) (98%, Wako), 1,1'-azobis(cyclohexane-1-carbonitrile) (V40) (98%, Wako), iodine (I_2) (>98%, TCI), tetrahydrofuran (THF) (>99.5%, Kanto, Japan), diethyl ether (>99.5%, TCI), chloroform (>

99.5%, TCI), methanol (>99.5%, TCI), acetonitrile (>99.5%, TCI), and diethylene glycol dimethyl ether (diglyme) (>99%, TCI) were used as received. Ethylene glycol bis(2-iodo-2-phenylacetate) (EPh-II) (Godo Shigen, Japan) and glycerol tris(2-iodoisobutyrate) (EMA-III) (Godo Shigen) were provided through the courtesy of Godo Shigen, Japan, and used as received. Deionized water was generated from an EMD Millipore Milli-Q™ Advantage A10 Water Purification System.

Measurement. The GPC analysis was performed on a Shimadzu LC-2030C Plus liquid chromatography (Tokyo, Japan) equipped with a Shodex (Tokyo, Japan) LF-804 mixed gel column (300 × 8.0 mm; bead size = 6 μm; pore size = 3000 Å) and a Shodex KF-804L mixed gel column (300 × 8.0 mm; bead size = 7 μm; pore size = 1500 Å). The eluent was THF at a flow rate of 0.7 mL/min (40 °C). Sample detection was conducted using a Shimadzu differential refractometer RID-20A. The column system was calibrated with standard poly(methyl methacrylate)s (PMMAs).

PDMI-I were purified with a preparative GPC (LC-9204, Japan Analytical Industry, Tokyo) equipped with JAIGEL 1H and 2H polystyrene gel columns (600×40 mm; bead size = 16 μm; pore size = 20-30 (1H) and 40-50 (2H) Å). Chloroform was used as eluent at a flow rate of 14 mL/min at room temperature.

The NMR spectra were recorded on a BBFO-400 spectrometer (400 MHz) (Bruker, Germany) at ambient temperature; ^{1}H: spectral width 4000.00 Hz, acquisition time 8.192 sec, and pulse delay 15.000 sec. The monomer conversion was determined from the peak area.

The DLS measurement was carried out on a Malvern Zetasizer Nano ZSP (Worcestershire, UK) at room temperature. The test angle for the DLS analysis was 173° (backscattering detection).

The TEM images were obtained on a JEM-1400 transmission electron microscope (JEOL) operated at 100 kV. The TEM grid was carbon-coated on 200 mesh (copper) (Ted

Pella, United States). The Cu grid was washed with acetone with sonication for 30 min before use.

General Procedure for Polymerization. In a typical run, a mixture of monomer (3 g), an alkyl iodide initiator, and a catalyst was heated in a Schlenk flask at 50-100 °C under argon atmosphere with a magnetic stirrer bar. After a prescribed time *t*, an aliquot (0.1 mL) of reaction solution was taken out by a syringe and cooled to room temperature. A portion of the aliquot was diluted by THF and analyzed by THF-GPC. The rest of the aliquot was diluted with $CDCl_3$ and analyzed with ^1H NMR for determining the monomer conversion.

Preparation of PDMI-I for NMR Analysis and Block Polymerizations. A mixture of DMI (12.7 g, 80 mmol), CP-I (0.16 g, 0.8 mmol), BNI (0.30 g, 0.8 mmol), and V65 (0.15 g, 0.6 mmol) was heated in a 100 mL flask at 60 °C under argon atmosphere with magnetic stirring. After 6 h, the mixture was cooled to room temperature and diluted with THF (10 mL). The polymer was reprecipitated in diethyl ether (100 mL), collected by filtration, and dried in vacuo to give a PDMI-I. For the NMR analysis (Figure 3), the polymer was further purified with the preparative GPC.

Preparation of PDMI-II for Block Polymerization. A mixture of DMI (3.2 g, 20 mmol), EPh-II (0.055 g, 0.1 mmol), and BNI (0.073 g, 0.2 mmol) was heated in a Schlenk flask at 60 °C under argon atmosphere with magnetic stirring. After 6 h, the mixture was cooled to room temperature and diluted with THF (3 mL). The polymer was reprecipitated in diethyl ether (30 mL), collected by filtration, and dried in vacuo to give a PDMI-II (monomer conversion = 16%) (M_n = 4400 and $Đ$ = 1.20 after purification).

Preparation of PDMI-III for Block Polymerizations. A mixture of DMI (3.2 g, 20 mmol), EMA-III (0.068 g, 0.1 mmol), and BNI (0.11 g, 0.3 mmol) was heated in a Schlenk flask at 60 °C under argon atmosphere with magnetic stirring. After 6 h, the mixture was cooled to room temperature and diluted with THF (3 mL). The polymer was reprecipitated in

diethyl ether (30 mL), collected by filtration, and dried in vacuo to give a PDMI-III (monomer conversion = 20%) (M_n = 9400 and $Đ$ = 1.25 after purification).

Preparation of PMMA–I for Block Polymerization. A mixture of MMA (3.0 g, 30 mmol), CP-I (0.059 g, 0.3 mmol), and BNI (0.11 g, 0.3 mmol) was heated in a Schlenk flask at 70 °C under argon atmosphere with a magnetic stirrer bar. After 0.5 h, the mixture was cooled to room temperature and diluted with THF (5 mL). The polymer was reprecipitated in hexane (60 mL), collected by filtration, and dried in vacuo to give a PMMA-I (monomer conversion = 20%) (M_n = 3700 and $Đ$ = 1.14 after purification).

Self-Assembly of Copolymers. A THF solution (0.2 mL) of a block copolymer (0.02 g) was added slowly into deionized water (1.8 mL) under stirring at room temperature (21 ^oC). The size of the assembly was studied with DLS after filtration (pore size = 450 nm). The solution (40 μL) was dropped on a Cu grid and dried under open air overnight for the TEM analysis.

2. Optimization of Polymerization Conditions for DMI.

Table S1. Polymerizations of DMI.

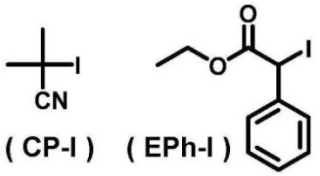

Oct_4NI (ONI)

Bu_3MePI (BMPI)

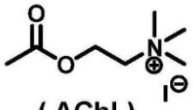

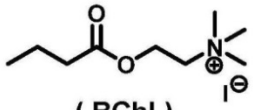

Entry	R-I	Catalyst	$[DMI]_0/[R-I]_0/[Cat]_0$ (mM)[a]	T / °C	t / h	M_n[b] ($M_{n,\,theo}$)[c]	$Đ$[b]	Conv / %
1	EPh-I	BNI	8000/80/80 (100/1/1)	60	45	3700 (1200)	1.32	8
2	CP-I	ONI	8000/80/80 (100/1/1)	60	48	4300 (2600)	1.36	16
3	CP-I	BMPI	8000/80/80 (100/1/1)	60	48	3600 (1900)	1.32	12
4	CP-I	AChI	8000/80/80 (100/1/1)	60	45	2200 (1200)	1.32	8
5	CP-I	BChI	8000/80/80 (100/1/1)	60	45	2100 (1000)	1.25	6

[a] Equivalents to R-I in the parenthesis. [b] PMMA-calibrated GPC values with tetrahydrofuran (THF) eluent. [c] Theoretical M_n values calculated according to $([M]_0/[R-I]_0)\times$(monomer conversion)$\times$(molar mass of monomer).

3. Synthesis of 3-Arm Block Copolymers.

A mixture of PPEGMA (1.2 g, 4 mmol), PDMI-III (DP = 20 (M_n = 9400 and $Đ$ = 1.25)) (0.094 g, 0.01 mmol), ONI (0.048 g, 0.08 mmol), V65 (0.0005 g, 0.002 mmol), and acetonitrile (0.8 g) was heated in a Schlenk flask at 60 °C under argon atmosphere with magnetic stirring for 3, 5, and 6 h. The GPC chromatograms are shown in **Figure S1**. The polymer was reprecipitated in diethyl ether, collected by filtration, and dried in vacuo.

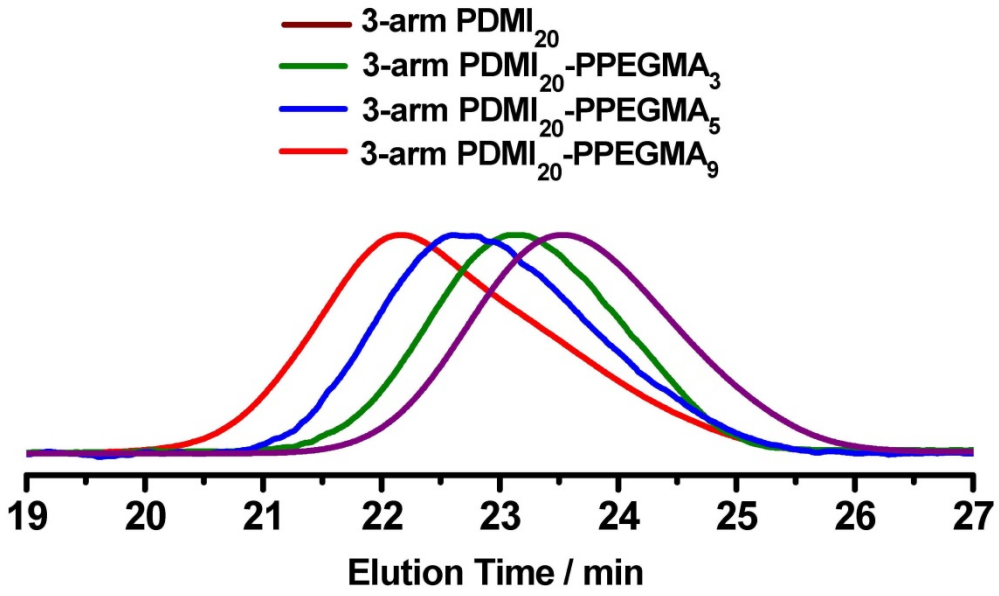

Figure S1. GPC traces of the 3-arm star block copolymers.